Simulation of the Acoustic Field of a Horn Loudspeaker by the Boundary Element – Rayleigh Integral Method

Stephen Kirkup, Ambrose Thompson, Bjørn Kolbrek and Javad Yazdani

S. M. Kirkup (Corresponding Author)
School of Computing, Engineering and Physical Sciences
University of Central Lancashire – West Lakes Campus
Samuel Lindow Building
Westlakes Science and Technology Park
Whitehaven
Cumbria
United Kingdom
CA24 3JY
smkirkup@uclan.ac.uk

(UK) (01946 51) 7200
A. Thompson
Martin Audio
Cressex Business Park
High Wycombe
Buckinghamshire
United Kingdom
HP12 3SL

Bjørn Kolbrek
Department of Electronics and Telecommunications
NO-7491 Norwegian University of Science and Technology
Trondheim
Norway

J. Yazdani
School of Computing, Engineering and Physical Sciences
University of Central Lancashire
Preston
Lancashire
United Kingdom
PR1 2HE

Running Title : Acoustic Field of a Horn Loudspeaker

Abstract

The boundary element – Rayleigh integral method (BERIM) is developed for the solution of acoustic problems consisting of a cavity with a single opening. The method is a hybrid of the interior boundary element method (BEM) and the Rayleigh integral method for the solution of the Helmholtz equation. FORTRAN codes for expressing the method for axisymmetric problems and general three-dimensional problems are developed. Both methods are applied to the problem of simulating the acoustic field produced by horn loudspeakers. The results are compared with measured data and the traditional exterior boundary element method. It is shown that the method can have significant computational advantages over the traditional BEM for problems consisting of an open cavity.

1. Introduction

The mathematical modelling and simulation of the acoustic field surrounding vibrating or scattering objects has always been a fundamental objective of acoustic engineers. Potentially we have a number of techniques that are available. For example for simple separable geometries we can often express analytic solutions. For more complicated (and practical) problems there are established numerical techniques such as the finite element method, finite difference method and the boundary element method (BEM).

The modelling of the acoustic field exterior or interior to a surface has received much attention. For both the interior and exterior problems, the BEM has the potential advantage over *domain methods* – such as the finite element and finite difference method – in that only the surface mesh is required. The BEM is also therefore particularly advantageous for exterior problems.

In both of the interior and exterior cases, the velocity potential (or sound pressure) in the domain can be related to the surface velocity and velocity potential through integral equations. The application of an integral equation solution method – or boundary element method – enables us to compute approximations to the sound pressure in the domain. The boundary element method is a well-established technique for interior and exterior acoustic problems, typical textbooks include Kirkup [1], Wu [2] and Ali and Rajakumar [3].

The purpose of this paper is to consider a particular class of acoustic problems; the determination of the acoustic field from a radiating cavity. Such problems can be viewed as *exterior* problems amenable to the exterior BEM. However, often the number of elements required to implement the exterior BEM in such cases is large, since the mesh

has to cover the interior and exterior back cover of the cavity at the same time, possibly leading to a relatively inefficient computational solution. An alternative method is to extend a *fictitious* boundary over each opening. This results in an exterior and an interior acoustic problem, which are coupled by the continuity of the acoustic field through the fictitious boundary. Such a method is considered in Seybert et al [4] and Polonio et al [5]. However, this method also requires both an interior and exterior mesh as well as a further mesh over the openings, and hence the number of elements is comparable to the direct application of the BEM and hence this is likely to be of similar efficiency.

The final approach, and the one that is examined in this paper, is to again place a fictitious boundary over an opening, and to couple the interior acoustic problem with the Rayleigh integral (that represents the exterior acoustic problem). The Rayleigh integral is a relatively simple equation that relates the exterior velocity potential to the surface velocity of a flat surface lying in an infinite baffle and it appears in many acoustics textbooks. Clearly there is not an infinite baffle at the cavity opening, and this method can only be used when there is one opening, but a mesh is only now needed for the interior and the opening of the cavity, hence there is a potential for efficiency savings, which will also be considered in this paper. The adoption of this model has the effect of also requiring that the fictitious boundary over the opening is flat.

A method based on this final approach was presented in Geddes et al [6], in which the finite element method is used to model the interior domain. In this paper the BEM is used to model the interior domain. The new method is called the boundary element – Rayleigh integral method (BERIM). The motivation for the exploration of this method is its application to the simulation of the sound field produced by a horn loudspeaker.

A horn loudspeaker is a type of acoustic transducer which presents to the vibrating piston a higher acoustic resistance than experienced by a piston in free air. The shape of the horn controls the degree of loading and directional characteristics.

Figure 1. W8LC Line Array, box and horn element. Highlighted section modelled.

Practical horns do not generally conform to the classical but are formed from geometry which prevents simple analysis. In professional sound reinforcement, horns have been an essential feature for many years [7]. Amongst its virtues are higher efficiency and a control over directional characteristics. The latter has become very important in recent years, due to the advent of high power amplifiers and compression drivers built to withstand them. It is for this reason that we concentrate on the SPL (sound pressure level) and polar response in this paper. The Boundary Element – Rayleigh Integral method is fist applied to an axisymmetric loudspeaker using the BERIMA program. For the general three-dimensional problem, the method BERIM3 is applied to the horn loudspeaker of figure 1 and results are presented for a wide range of sample frequencies.

2. The Boundary Element – Rayleigh Integral Model

An illustration of the sort of problems that are considered in this paper in two dimensions is shown in figure 2, where the acoustic domain E is exterior to the c-shaped surface. Clearly the smaller the opening the more the 'interior' part gets closer to a closed cavity model.
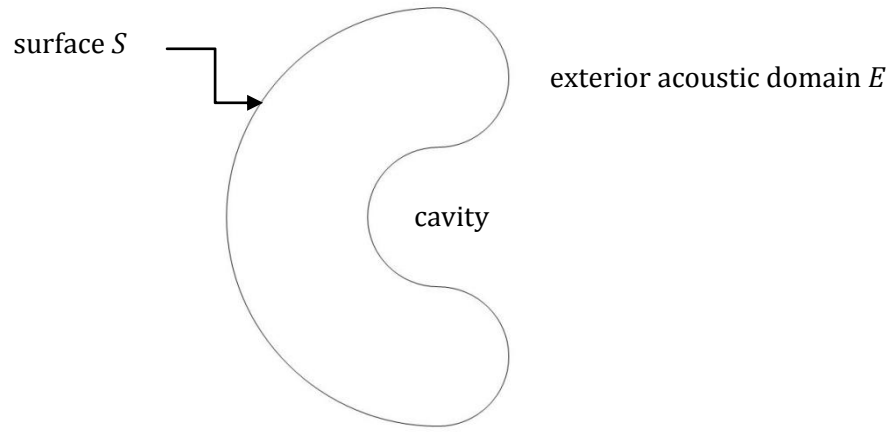

Figure 2. Illustration of an open cavity.

For a typical acoustic domain, such as air or water, the acoustic field can be modelled by the wave equation that can be written as a sequence of Helmholtz problems, each with a different wavenumber k:

$$\nabla^2 \varphi(\mathbf{p}) + k^2 \varphi(\mathbf{p}) = 0 \quad (\mathbf{p} \in E) \qquad (1)$$

where $k = \frac{\omega}{c} = \frac{2\pi\nu}{c}$ where ν is the frequency in Hz, ω is the angular frequency and c is the speed of sound, φ is the velocity potential, related to the sound pressure p at a point $\mathbf{p}$ by the formula $p(\mathbf{p}) = i\rho\omega(\mathbf{p})\varphi(\mathbf{p})$, where ρ is the density of the acoustic medium.

If we return to the choice of appropriate simulation techniques, we know that interior and exterior acoustic problems can be typically analysed by the finite element method (FEM) or boundary element method (BEM). For the interior problem the FEM is a well-established technique, which requires a mesh of the whole domain, whereas the BEM only requires a mesh of the boundary. For the exterior problem, the FEM is more difficult to apply because of the large (or infinite, as modelled) domain, whereas again the BEM only requires a boundary mesh. Hence the BEM is an attractive method of solution for typical acoustics problems. There are a number of papers considering the application of the BEM to loudspeaker structures [8-12], and particularly a horn loudspeaker [13].

Illustrated on the two-dimensional domain, applying the exterior BEM to the cavity problem would first require a mesh of the boundary, as illustrated in figure 3.
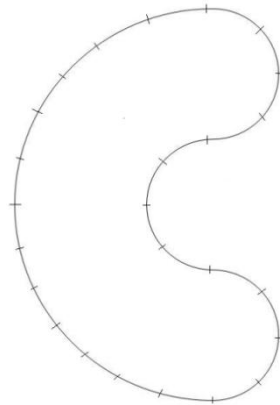

Figure 3. BEM mesh for the open cavity.

The application of the BERIM method to this problem involves a revision in the model of the domain so that it consists of two separate regions; an *interior* region consisting of the cavity and an *exterior* region beyond a plane at the opening. In the application of the BERIM method, a mesh is only required in the cavity and in the opening of the cavity, as

7

illustrated in figure 4. It can be seen that the number of elements required in the BERIM method is substantially less than the number of elements required in the BEM mesh in figure 3 and there is a much greater potential for reducing the number of elements in typical general three-dimensional problems. In order to complete the model we couple the interior and exterior fields by simply applying the condition that the acoustic field is continuous across the opening.
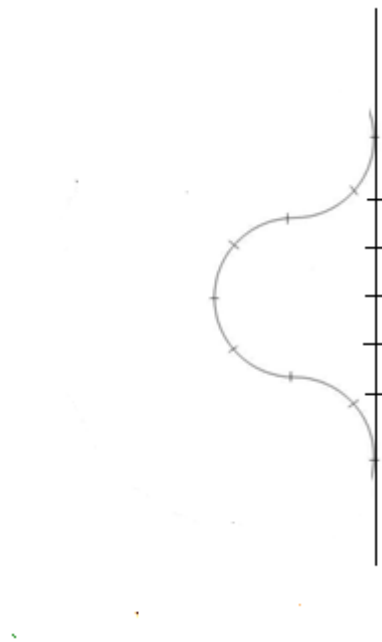
Figure 4. BEM mesh for the BERIM method applied to the cavity.

Clearly the choice of the BERIM method effectively alters the nature of the acoustic domain, but this must be weighed against the potential benefit of having a smaller mesh; potentially resulting in a more efficient method and reducing the effort in defining the mesh. For many loudspeakers, the front of the cabinet is a natural finite baffle and in such cases the BERIM method is expected to provide a suitable model.

3. The Boundary Element – Rayleigh Integral Method

In this section a mathematical derivation of the Boundary Element – Rayleigh Method using the typical concepts and notation found in the Boundary Element Method [1]. Let S be the surface of the cavity and Π be the opening. The boundary condition is applied on the surface of the cavity and the condition is presumed to be most generally in the following form:

$$a(\mathbf{p})\varphi(\mathbf{p}) + b(\mathbf{p})v(\mathbf{p}) = f(\mathbf{p}) \qquad (\mathbf{p}\in S) \qquad (2),$$

although for the horn loudspeaker application in this work only the Neumann condition is considered: $a(p)=0$, $b(p)=1$ ($\mathbf{p}\in S$).

The BERIM method is derived through coupling the interior boundary integral equation formulation for points on interior Helmholtz equation for the cavity [1],

$$\{M_k + \frac{1}{2}I\}_{S+\Pi}\varphi(\mathbf{p}) = \{L_k\}_{S+\Pi}v(\mathbf{p}) \quad (\mathbf{p}\in S{+}\Pi), \quad (3)$$

and the Rayleigh integral for points on Π [14],

$$v(\mathbf{p}) = -2\{L_k\}_{\Pi}\varphi(\mathbf{p}) \quad (\mathbf{p}\in \Pi). \qquad (4).$$

In equations (2) and (3), φ represents the velocity potential and v its derivative with respect to the normal that is outward to the cavity. The operators are defined as follows:

$$\{L_k\mu\}_{\Gamma}(\mathbf{p}) = \int_{\Gamma} G(\mathbf{p},\mathbf{q})\mu(\mathbf{q})dS_q \text{ and } \{M_k\mu\}_{\Gamma}(\mathbf{p}) = \int_{\Gamma} \frac{\partial G(\mathbf{p},\mathbf{q})}{\partial n_q}\mu(\mathbf{q})dS_q$$

where G is the free-space Green's function for the Helmholtz equation and Γ is used here to represent any surface or part of the surface (including Π), I is the identity operator.

If we consider equation (3) for points on S and Π separately then we obtain the following equations:

$$\{M_k + \frac{1}{2}I\}_S \varphi(\mathbf{p}) + \{M_k\}_\Pi \varphi(\mathbf{p}) = \{L_k\}_S v(\mathbf{p}) + \{L_k\}_\Pi v(\mathbf{p}) \quad (\mathbf{p} \in S) \quad (5)$$

$$\{M_k\}_{S+\Pi} \varphi(\mathbf{p}) + \{M_k + \frac{1}{2}I\}_\Pi \varphi(\mathbf{p}) = \{L_k\}_S v(\mathbf{p}) + \{L_k\}_\Pi v(\mathbf{p}) \quad (\mathbf{p} \in \Pi) \quad (6)$$

The computational method is applied by meshing the interior surface of the cavity and the opening alone. By approximating φ and v by constants on each element and through collocation of the integral equations, (4), (5), and (6) can be written as linear systems of equations:

$$\underline{v}_\Pi = -2[L_k]_{\Pi\Pi} \underline{\varphi}_\Pi \qquad (7),$$

in line with the Rayleigh Integral Method [15], and

$$[M_k + \frac{1}{2}I]_{SS} \underline{\varphi}_S + [M_k]_{S\Pi} \underline{\varphi}_\Pi = [L_k]_{SS} \underline{v}_S + [L_k]_{S\Pi} \underline{v}_\Pi \qquad (8),$$

$$[M_k]_{\Pi S} \underline{\varphi}_S + [M_k + \frac{1}{2}I]_{\Pi\Pi} \underline{\varphi}_\Pi = [L_k]_{\Pi S} \underline{v}_S + [L_k]_{\Pi\Pi} \underline{v}_\Pi \quad (9)$$

respectively, in line with the standard interior boundary element method [1]. The correspondence between (4-6) and (7-9) should be clear. The operators L_k, M_k and I are replaced by the matrices $[L_k]$, $[M_k]$ and $[I]$ and the boundary functions φ and v are replaced by vectors of data $\underline{\varphi}$ and $\underline{v}$.

In the collocation method the centres of the elements, the collocation points, are the representative points on the cavity surface and opening at which the surface functions φ and v are observed. If the cavity surface S is divided into n elements and opening Π is divided into m elements then $\underline{\varphi}_S$ is an n-vector, $\underline{\varphi}_\Pi$ is a m-vector, $[L_k]_{S\Pi}$ is an nxm matrix etc. With equations (7-9) we then have *n+2m* equations with potentially *2n+2m*

unknowns. The system is completed with the n equations that are provided by the discrete form of the boundary condition (1),

$$[D_a]_{SS}\,\underline{\varphi_S}+[D_b]_{SS}\,\underline{v_S} = \underline{f_S} \qquad (10)$$

where $[D_a]_{SS}$ and $[D_b]_{SS}$ are diagonal nxn matrices with the diagonal made up of the values of $a(\mathbf{p})$ and $b(\mathbf{p})$ at the collocation points on S.

Using equations (7-10) we can form a *(2n+2m)x(2n+2m)* system of equations that returns approximations to the values of φ and v at the collocation points. For purely Neumann or Dirichlet boundary conditions we can simplify (9) and in these cases we can write the coupled system as an (n+2m)x(n+2m) system.

Once the surface functions are determined, results on the cavity D can be found using the integral

$$\varphi(\mathbf{p}) = \{L_k\}_{S+\Pi}\,v(\mathbf{p}) - \{M_k\}_{s+\Pi}\,\varphi(\mathbf{p}) \quad (\mathbf{p}\in D), \qquad (11)$$

and the Rayleigh integral can be used again for points in the exterior E

$$v(\mathbf{p}) = -2\{L_k\}_{\Pi}\,\varphi(\mathbf{p}) \quad (\mathbf{p}\in E) \qquad\qquad (12).$$

In all cases the discrete operators are evaluated using the methods and codes H3LC and H3ALC, described in Kirkup [15], [1].

The Boundary Element – Rayleigh Integral method (BERIM) is implemented in two distinct ways, applied to suitable horn loudspeaker test problems and results are given. Firstly the method is applied to axisymmetric problems (BERIMA) in the next section and secondly the general three-dimensional method (BERIM3) in section 4.

4. BERIMA: The Axisymmetric Method, Test Problem and Results

For axisymmetric problems, it is assumed that the cavity, the boundary condition and the acoustic field have rotational symmetry. Clearly this represents a particular class of problems, but the inherent simplifications allow us to reduce the number of elements

significantly, and the method has the important property of allowing us to explore the properties of the BERIM at a reduced computational cost. The method is extended to the more general acoustic problem in the next section.

For the axisymmetric case, the surface of the cavity is divided into truncated conical elements, the opening is respresented by a set of annular rings, and the acoustic properties are represented by a constant on each element, in line with the general development of boundary element method [1].

4.1 Comparison of BERIMA results with measured data

The BERIMA routine was tested by applying it to the design of an actual axisymmetric horn loudspeaker. One of the authors (Kolbrek) contributed to the design of an axisymmetric horn for midrange use, and AEBEMA and BERIMA was used in the design process. The horn is calculated according to a method developed by Jean-Michel Le Cléac'h. In this method, the wave front areas are calculated according to the general family of hyperbolic-exponential horns [17], but the horn profile is corrected to take the curving of the wave fronts into account. A more detailed description of the method is given in [18] (in French), where also a spreadsheet to calculate the profile can be downloaded [19]. As far as the authors are aware, this horn has not been investigated in the professional literature before. As can be seen from the simulations and measurements, this horn does not have particularly good directivity control, but the acoustical impedance at the entrance (throat) of the horn, is exceptionally smooth.

The horn used in this comparison has the following parameters: cut-off frequency 425Hz, throat radius 17.8mm, and parameter T = 0.71. The parameters were chosen obtain a good match to the Altec 288 series of compression drivers.

As the boundary for the axisymmetric methods are represented as truncated conical shells, generating the vertices is very simple. A dedicated pre-processor incorporating a horn profile generator was implemented, generating the mesh shown in figure 5. The rectangles show the vertices. The line shown to block the large end of the horn is the part of the mesh used in the RIM part of the BERIM method. The rule-of-thumb of 6 elements per wavelength was used in setting the vertex spacing. The normal velocity was set to 1m/s at the throat (assumed to be flat), and zero everywhere else.
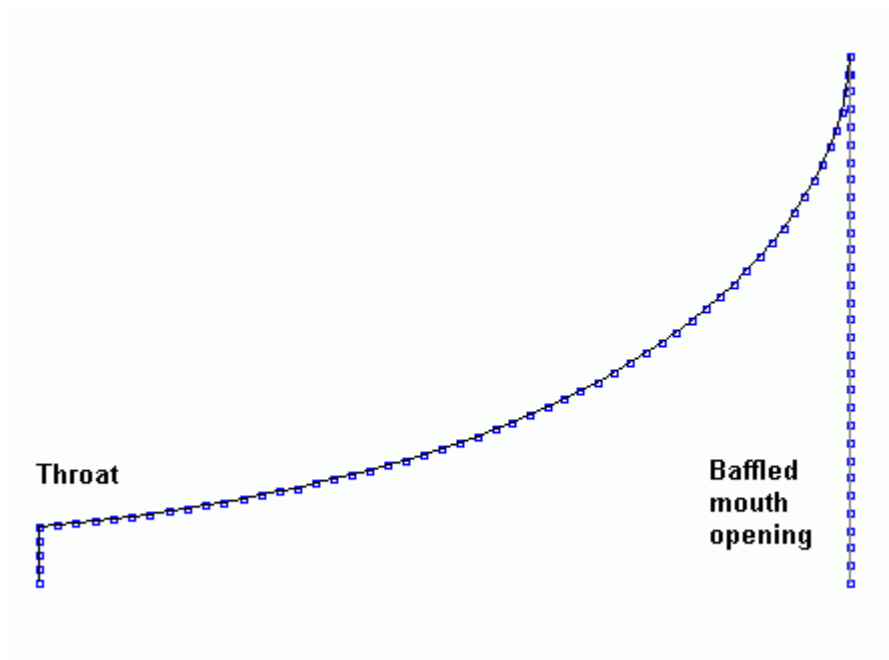

Figure 5. BERIMA boundary for test horn

The field points for directivity simulations were placed along the quarter of a circle of 3 meters radius, covering 0-90 degrees. 91 field points were used to get good resolution. For directivity simulations, 15 frequencies logarithmically spaced from 400Hz to 10kHz were used. A polar map, showing the directivity response at all frequencies as level contours, is shown in figure 6. The measured response of the horn is shown in figure 7. In both cases the response is normalized to the on-axis response. The horn was measured without a baffle, which affects the results mainly at low frequencies. At higher

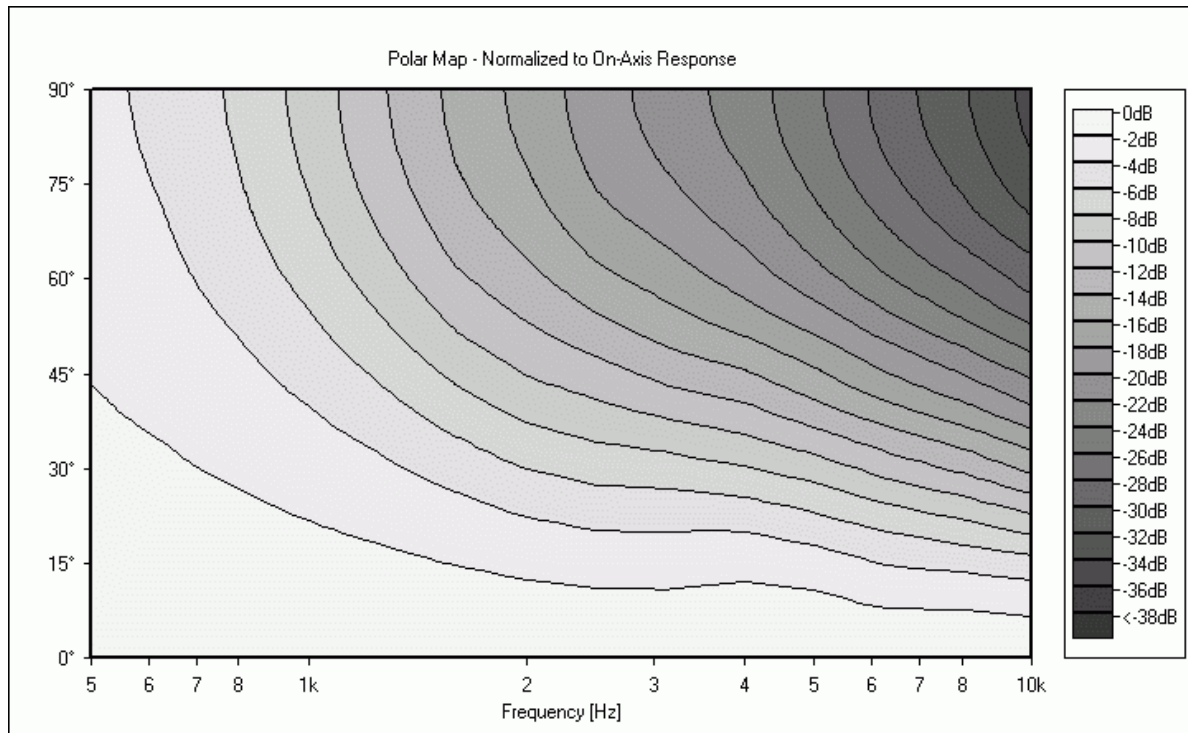frequencies, where the horn is somewhat more directive; the differences are less marked.

Figure 6. Simulated directivity response of the test horn using BERIMA.
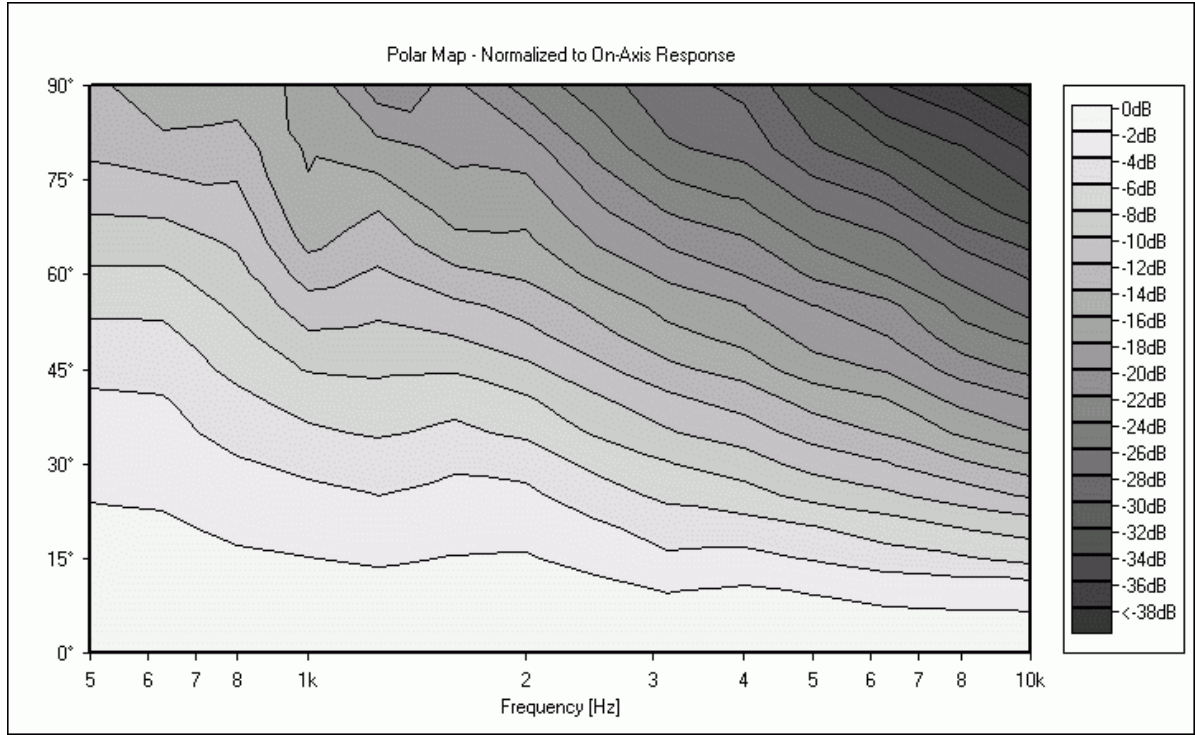
Figure 7. Measured directivity response of the test horn.

The throat impedance of the horn was also simulated. The knowledge of the throat impedance is important if it is desired to calculate the combined response of the horn-driver combination. The throat impedance will also give information about reflections present in the horn. Reflections will give rise to standing waves or resonances in the horn, which will show up as ripple in the throat impedance. The throat impedance is defined as the complex ratio of pressure to volume velocity. Here it is calculated as the average impedance over the elements making up the throat, as

$$Z_{th} = \sum_{\text{throat elements}} \frac{p_i}{u_i A_i}$$

where i is the index of the throat elements p_i, u_i and A_i being the pressure, velocity and surface area of each element respectively. To get a good impression of the throat

impedance, rather more than 15 frequencies are required, but no field points are needed.

In this investigation, 150 frequencies, logarithmically spaced from 100Hz to 10kHz were used. The throat impedance of the test horn was measured using the single-microphone of Salava [20] A comparison of the throat impedance simulated by BERIMA and the impedance measured on the actual horn is shown in figures 8 (resistance) and 9 (reactance). The curves have been normalized by multiplying the actual values by $\frac{S_t}{\rho c}$, where S_t is the throat area. The deviation is greatest around the cut-off frequency, the reason for this is the differences in mouth terminating conditions (2π vs. 4π solid angle). Note that the theoretically better terminated horn has more ripple than the horn radiating into full-space, indicating somewhat more reflection from the mouth. Repeated simulations have shown that this is normal for this horn type, and is believed to be caused by differences in the way the waves expand outside the horn. The horn contour will, if continued beyond the plane of the baffle, roll back gently, and it appears that this will cause less reflection back into the horn.

Note also the peaks around 6kHz for the measured throat impedance. These peaks correspond to the first radial mode of the impedance tube used in the measurements, which has an inner diameter of 35.6mm. The peaks around 8-9kHz may be the result of the second mode, but may also be a result of angular modes in the tube, as a result of non-axisymmetric wave propagation, as the second radial mode would occur at about 10kHz.
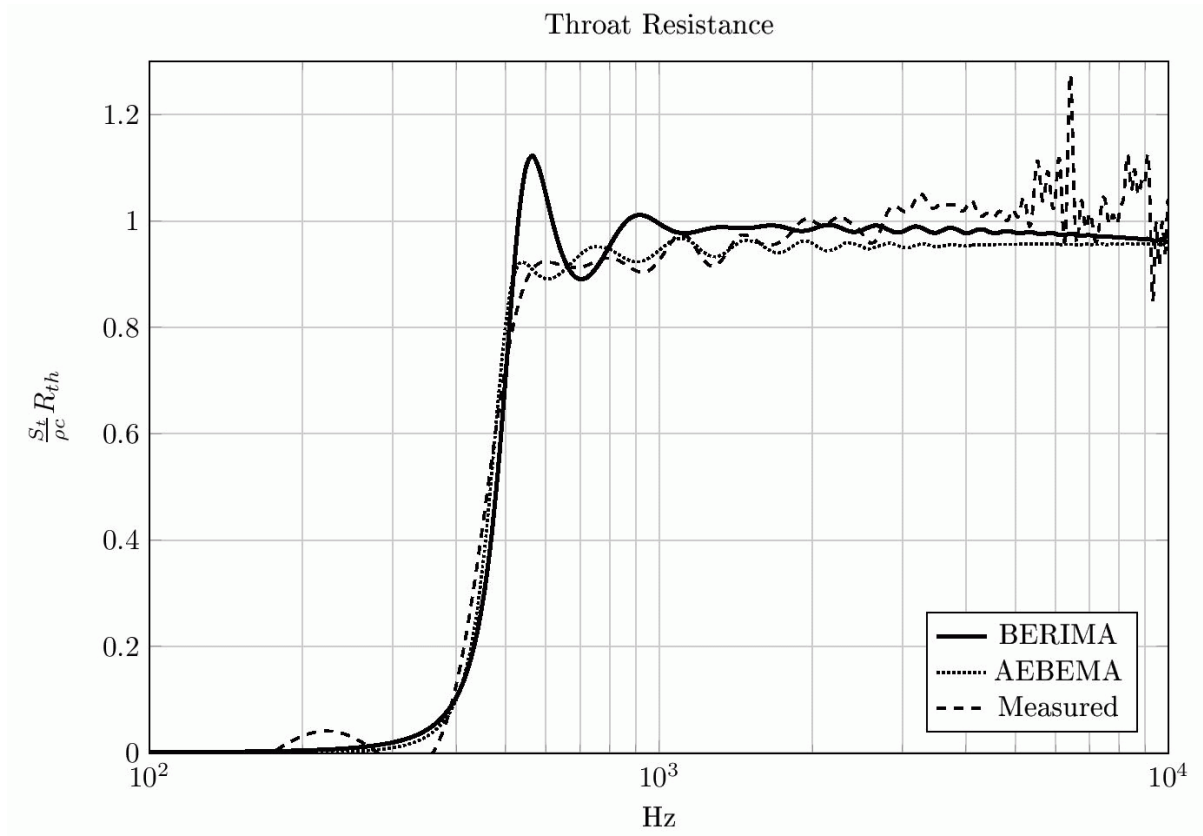
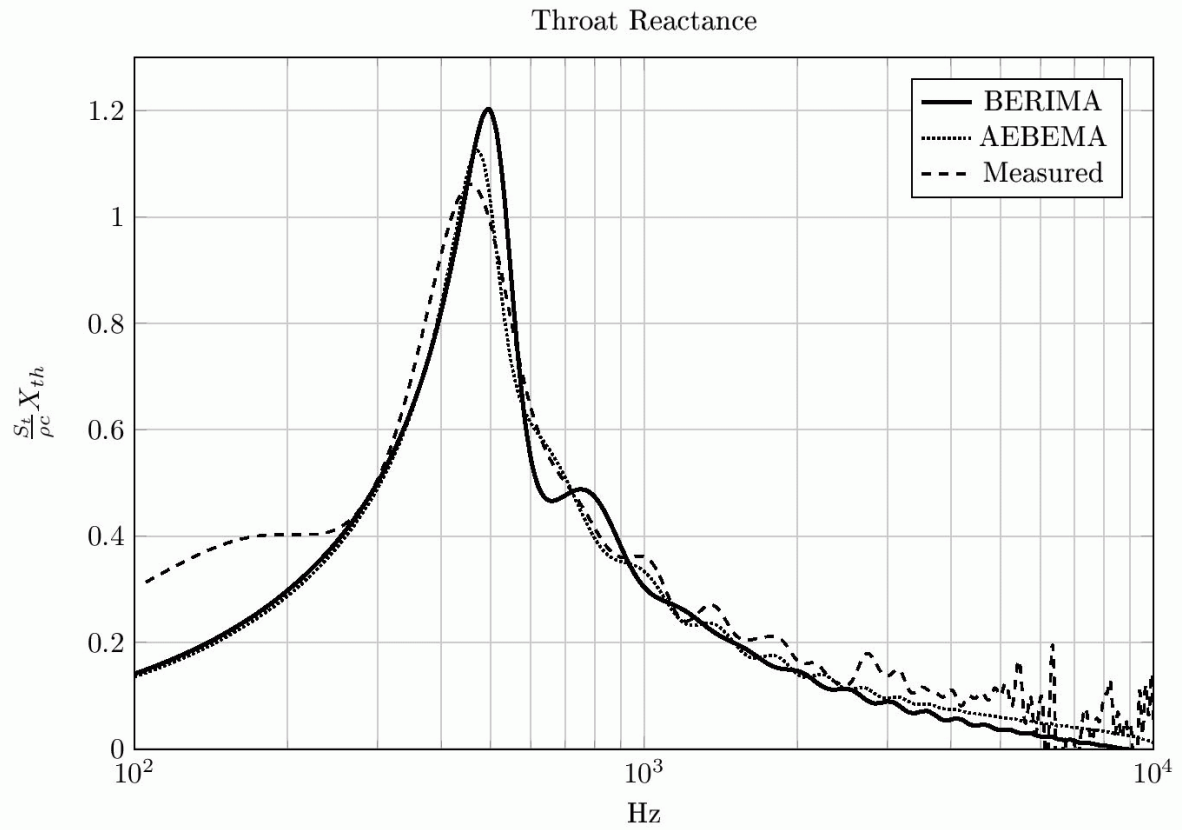Figure 8. Throat resistance, comparison of BERIMA, AEBEMA and measured values.

Figure 9. Throat reactance, comparison of BERIMA, AEBEMA and measured values

4.2 Comparison of BERIMA results with those from the AEBEMA boundary element code.

For further validation of BERIMA, and to investigate possible improvements in computer run times, the same horn was simulated with AEBEMA [1], using the ordinary boundary elements method. The horn was placed in a cylinder to create a complete, closed boundary. The mesh size of the cylinder was chosen to be twice the size of mesh size in the horn. This had previously been found to have very little effect on the calculated results, and was done to reduce computer run times. The distance between the horn throat and the back wall is set to be a little larger than the length of one typical element, as a compromise between not making the mesh unnecessarily large, and not making the structure too thin. The mesh for the AEBEMA code is shown in figure 10. Both directivity and throat impedance was simulated at the same frequencies as was used for BERIMA.
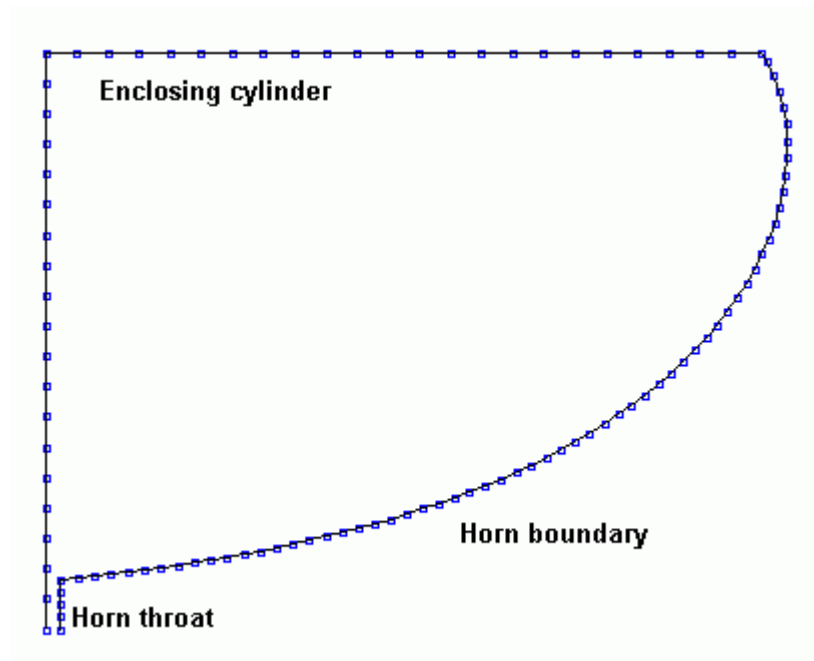

Figure 10. AEBEMA boundary for test horn.

The polar map for the horn simulated using AEBEMA is shown in figure 11. The throat impedance is shown in figures 8 and 9, where it is compared to BERIMA and measurements.
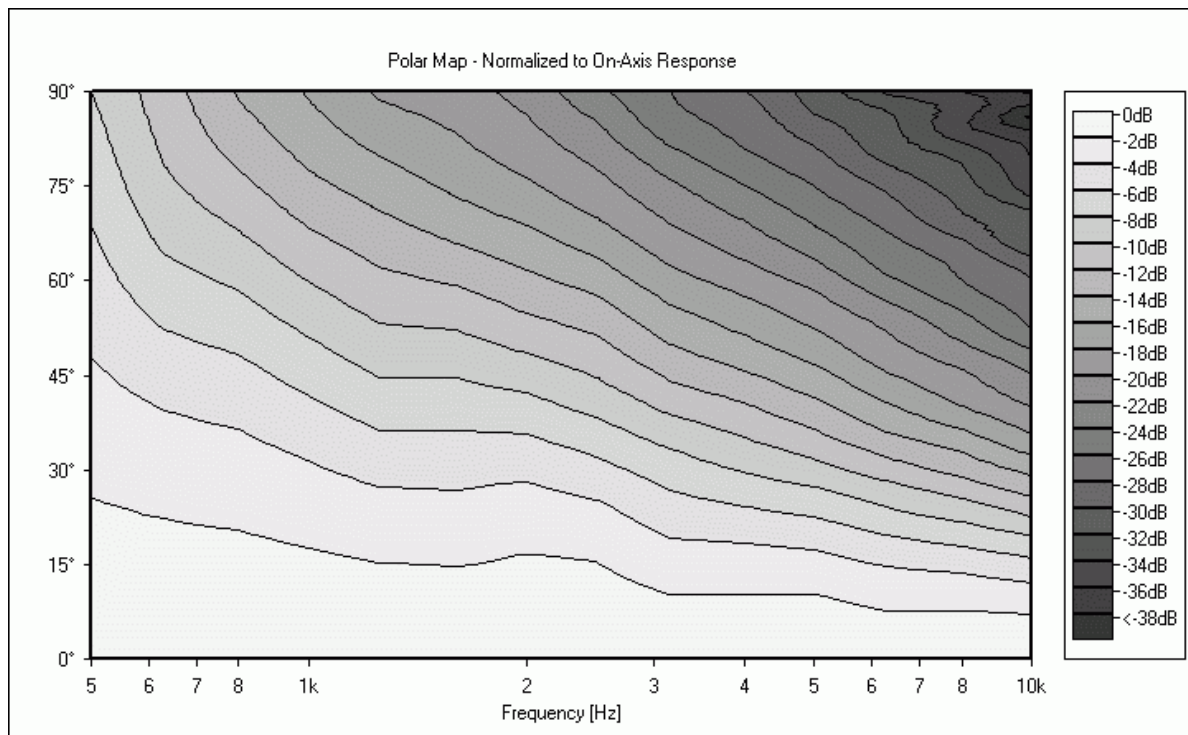

Figure 11. Simulated directivity response of test horn using AEBEMA.

BERIMA was found to be significantly faster than AEBEMA for the test problem considered in this subsection. Table 1 compares the programs for the test problem All calculations were done on a computer having an Intel Pentium 4, 3.0GHz processor and 1.0GB RAM. The speed advantage of BERIMA is evident.

	BERIMA	AEBEMA
Number of elements	88	107
Ratio of max to min element radial size	1.36	3.25
Directivity calculation time	7m 36s	21m 52s
Impedance calculation time	33m 15s	2hr 41m, 16s

Table 1: Comparison of BERIMA and AEBEMA

5. BERIM3: The General 3D Method, Test Problem and Results

One of the authors (Thompson) applied the general three-dimensional method to a horn loudspeaker, similar to the ones illustrated in figure 1 [21]. In order to apply BERIM3 to the horn loudspeaker, first the 3D solid model is generated automatically from a set of around 10 parameters. The model is then introduced into the popular GID pre/post processor [22] where a triangulation of the interior surface and mouth is made and subsequently solved. A typical GID post process mesh is shown in figure 12. A velocity of 1m/s was set at the "throat" (assumed to be flat) and zero everywhere else. In order to mitigate the numerical effects of the sudden change in boundary conditions where the cavity surface meets the mouth, a small flange was added. A record of each calculation can be found in table 1, where number of elements and approximate running time on a AMD2200 PC platform are given.
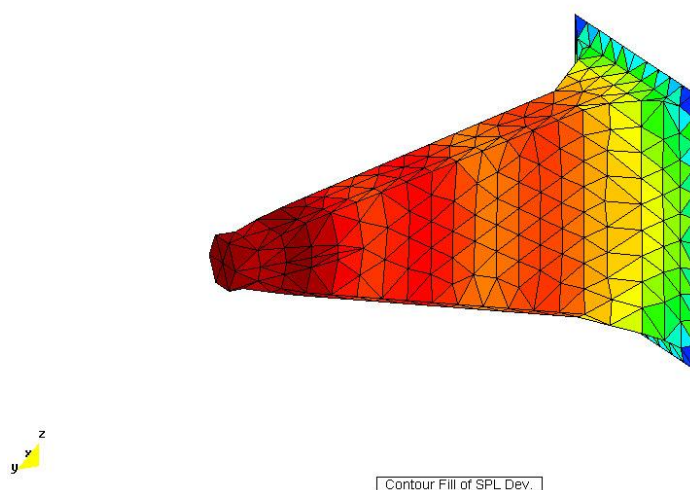

Contour Fill of SPL Dev.

Figure 12. Typical BERIM3 mesh showing surface SPL at 3kHz

5.1 Comparison of BERIM3 results with measured data

The sound pressure is observed on polar paths of 1m radius. The results from BERIM3 are compared with measured results in figure 13, showing polar plots of the sound pressure level (SPL) in the vertical and horizontal polar plane and an illustration of the mouth velocity amplitude for 3, 6, 9, 12,and 15kHz.
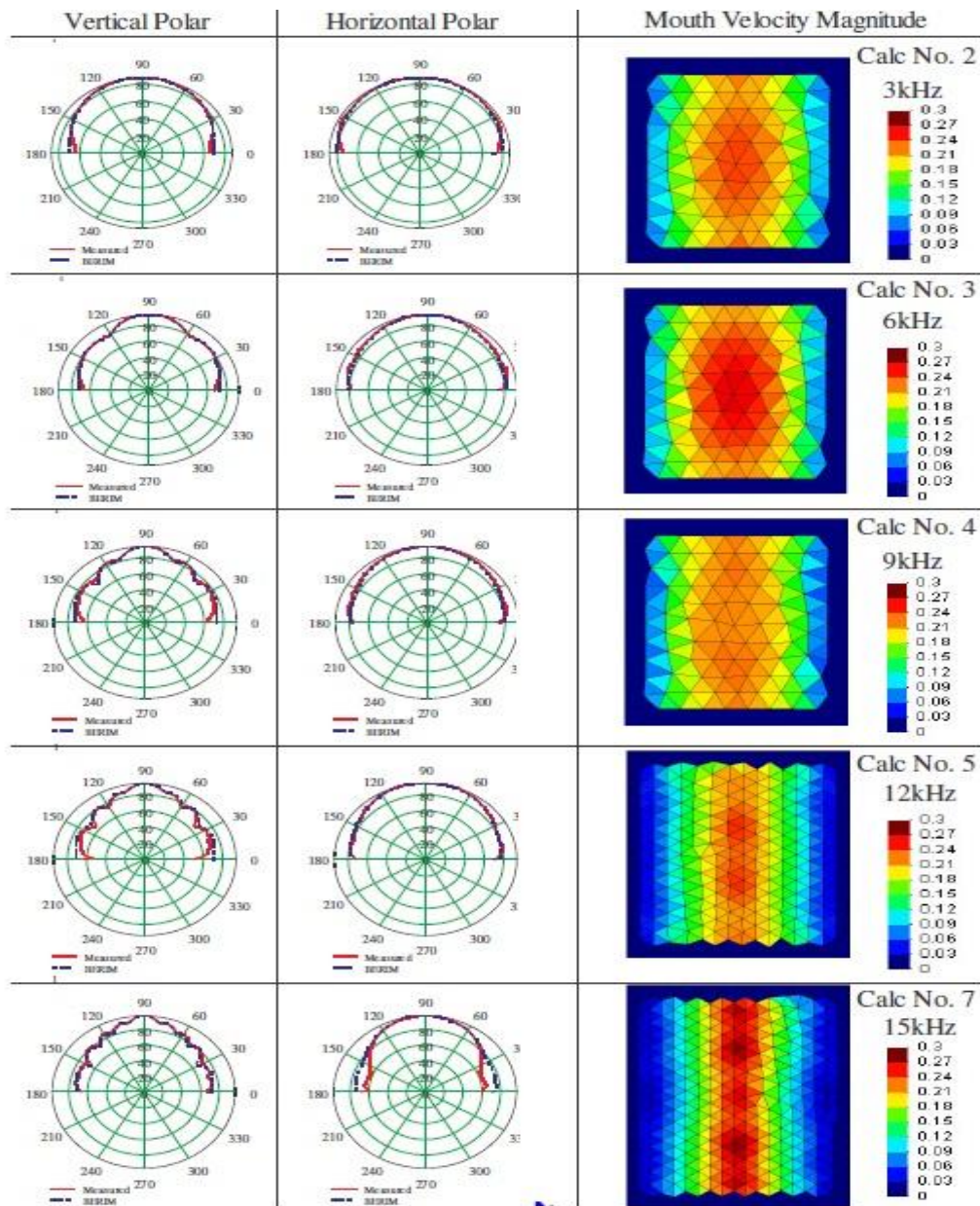

Figure 13. Comparison of computed and measured polar plots and computed SPL at the mouth.

5.2 Comparison of BERIM3 results with those from the AEBEM3 boundary element code.

By way of comparison and further validation, the application of BERIM3 is compared with the application of the boundary element method (AEBEM3) to the same problem, but at 3kHz only. In order to apply the BEM, the mesh in figure 14 is used. The horizontal and vertical polar plots of the SPL at 1m is shown in figure 15. A comparison of typical computer run times for the BERIM and BEM methods for the 3D problem is given in table 2.
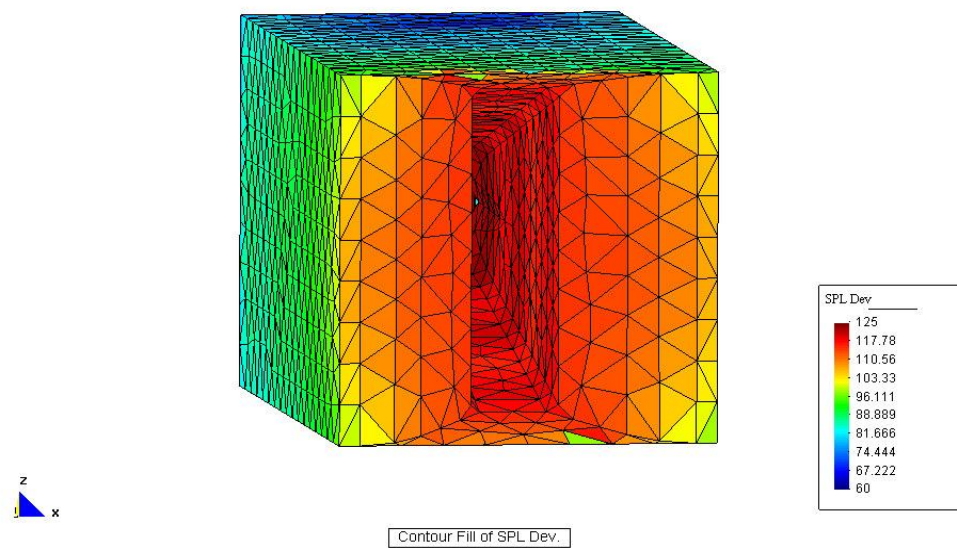

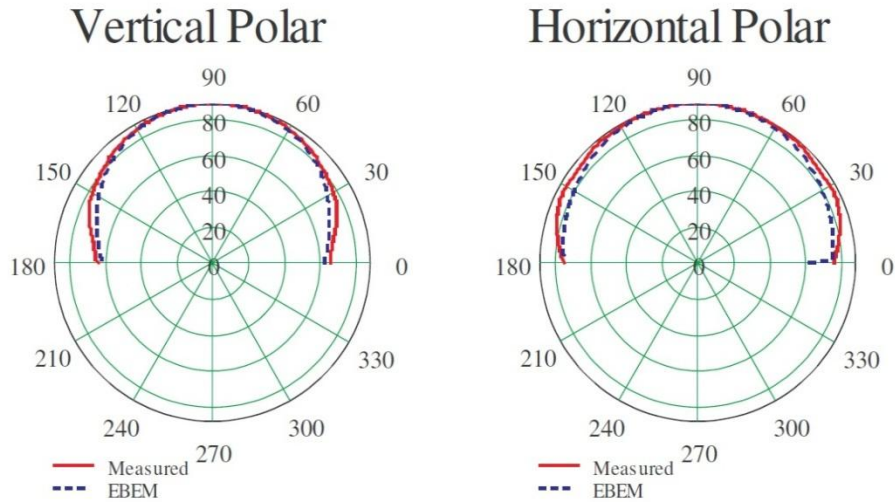Figure 14. BEM mesh showing sound pressure level at 3kHz.

Figure 15. Comparison of BEM results with measured data.

Calculation	Solver	Freq	Element Size	Num Elements	Time
1	AEBEM	3kHz	12mm	2189	23min
2	BERIM	3kHz	12mm	994	2min
3	BERIM	6kHz	12mm	994	2min
4	BERIM	9kHz	12mm	994	2min
5	BERIM	12kHz	8mm	2035	25min
6	BERIM	12kHz	7mm	2600	56min
7	BERIM	15kHz	7mm	2600	56min

Table 2. Comparison of BERIM3 and AEBEM3 computer run times.

6. Conclusion

For a structure such as a horn loudspeaker, which consists of a cavity (the horn) opening out on to the front of a cabinet, the Boundary Element – Rayleigh Integral Method (BERIM) seems most applicable. In the illustrative domain in figure 4, and in the axisymmetric test problems in figure 5 and the general test problem in figure 12 it is shown that BERIM requires a mesh of the interior surface and opening plane alone, whereas the application of the boundary element method (BEM) to the same problem requires considerably more elements, as shown in figures 10 and 14. As well as the

reduction in the number of elements, two other factors help to reduce the computer run times; firstly fewer operators require discretisation in the BERIM, method and when calculating the values at the external field points, only the velocity distribution at the mouth has to be taken into account, not the entire boundary.

Hence, in many situations when it can be applied, the BERIM reduces the meshing required and typically uses an order of magnitude less computer time than the straightforward BEM. The directivity response for the axisymmetric horn shows good agreement between BERIM results, measured results and BEM results and the polar plots for the general 3D horn show good agreement with measured results in figure 13 and with BEM results in figure 14.

For the general 3D case, BERIM3 seems to give better agreement with measured than the BEM in the forward field, however, near the baffle the BEM has more agreement. The proposed reason for this is that the BEM accurately meshes the baffle whereas BERIM assumes and infinite baffle; BERIM3 gives more support to the wider field than the true finite baffle. In general the lobes in the sound field are captured. There is only significant drift in the horizontal polar at 15kHz: this would probably benefit from a further refinement in the mesh.

In general the Boundary Element – Rayleigh Integral method is a useful additional technique for the simulation of the sound field of a horn loudspeaker or other acoustic problems consisting of a cavity with one opening, which can return a significant reduction in computation time. The codes BERIM3 and BERIMA, introduced in this paper, as well as the other codes AEBEM3 and AEBEMA, and the supporting codes are available as open source [1].

References

[1] S. M. Kirkup, "The Boundary Element Method in Acoustics", 1998, Integrated Sound Software 2007. pp1-160. Website containing electronic book and downloadable software - http://www.boundary-element-method.com. (date last viewed 24/11/11)

 [2] T. W. Wu (ed), "Boundary Element Acoustics: Fundamentals and Computer Codes", Wessex Institute of Technology Press, 2000, pp1-150.

[3] A. Ali, C. Rajakumar, "Boundary Element Method: Applications in Sound and Vibration", Taylor & Francis, 2007, pp1-198.

[4] A. F. Seybert, C. Y. R. Cheng and T. W. Wu, "The solution of coupled interior/exterior acoustic problems using the boundary element method", J. Acoust. Soc. Am. 88(3), 1612-1616, (1990).

[5] F. Polonio, T. Loyau, J-M Parot and G. Gogu, "Acoustic Radiation of an Open Structure: Modeling and Experiments", Acta Acustica united with Acustica, 90(3), 2004.

[6] E. Geddes, J. Porter and Y. Tang, "A Boundary-Element Approach to Finite-Element Radiation Problems", J. Audio Eng. Soc. **35**(4), 1987

[7] Martin Audio (2004) Website – Historical and Product information www.martin-audio.com (date last viewed 24/11/11)

[8] C. J. C. Jones, "Finite Element Analysis of Loudspeaker Diaphragm Vibration and prediction of the Resulting Sound Radiation", PhD Thesis, Brighton Polytechnic, 1986.

[9] S. M. Kirkup and M. A. Jones, "Computational methods for the acoustic modal analysis of an enclosed fluid with application to a loudspeaker cabinet", Applied Acoustics, **48**(4), 1996, pp 275-299

[10] K.J.Bastyr, D.E.Capone, "On the Acoustic Radiation from a Loudspeaker's Cabinet" J. Audio Eng. Soc, **51**(4), pp 234- 243, 2003

[11] E. F. Grande, "Sound Radiation from a Loudspeaker Cabinet using the Boundary Element Method", Master Thesis, Technical University of Denmark, 2008.

[12] J. Vanderkooy and D. J. Henwood, "Polarplots at low frequencies: The acoustic centre", Audio Engineering Society convention paper, 6784, 120th Convention, Paris, France, 2006

[13] D. J. Henwood, "The Boundary – Element Method and Horn Design", J. Audio Eng. Soc, **41**(6), pp 485- 496, 1993.

[14] S. M. Kirkup, "Computational solution of the acoustic field surrounding a baffled panel by the Rayleigh integral method", Applied Mathematical Modelling, **18**(7), pp 403-407 , 1994

[15] S. Kirkup, "Fortran codes for computing the acoustic field surrounding a vibrating plate by the Rayleigh integral method", Proceedings of the conference on MATHEMATICAL METHODS, COMPUTATIONAL TECHNIQUES AND INTELLIGENT SYSTEMS (MAMECTIS '08), Corfu, Greece, October 26-28, 2008. pp46-52.

[16] S. M. Kirkup, "Fortran codes for computing the discrete Helmholtz integral operators", Advances in Computational Mathematics, vol. 9, no. 3/4, pp. 391-409, 1998.

[17] V. Salmon, "A New Family of Horns", JASA, vol. 17, Jan. 1946, pp. 212-218.

[18] Calcul des pavillons par éléments discrets (Calculation of flats by discrete elements), http://ndaviden.club.fr/pavillon/lecleah.html (date last viewed 30/11/11)

[19] B. Kolbrek, "Horn Theory: An Introduction, Part 2", AudioXpress, 2008, pp. 20-29.

[20] T. Salava, "Measurement of the Input Impedance of Horns", J. Audio Eng. Soc., Vol. 29, No. 6, 1981, pp. 416-420.

[21] S. Kirkup and A. Thompson, "Computing the Acoustic Field of a Radiating Cavity by the Boundary Element - Rayleigh Integral Method (BERIM)" , Proceedings of the World Congress on Engineering 2007 Vol II, WCE 2007, July 2 - 4, 2007, London, U.K.

[22] GID Pre/Post processor http://www.gidhome.com/ (date last viewed 24/11/11)

	BERIMA	AEBEMA
Number of elements	88	107
Ratio of max to min element radial size	1.36	3.25
Directivity calculation time	7m 36s	21m 52s
Impedance calculation time	33m 15s	2hr 41m, 16s

Table 1: Comparison of BERIMA and AEBEMA

Calculation	Solver	Freq	Element Size	Num Elements	Time
1	AEBEM	3kHz	12mm	2189	23min
2	BERIM	3kHz	12mm	994	2min
3	BERIM	6kHz	12mm	994	2min
4	BERIM	9kHz	12mm	994	2min
5	BERIM	12kHz	8mm	2035	25min
6	BERIM	12kHz	7mm	2600	56min
7	BERIM	15kHz	7mm	2600	56min

Table 2. Comparison of BERIM3 and AEBEM3 computer run times.

Figures captions

Figure 1. W8LC Line Array, box and horn element. Highlighted section modelled.

Figure 2. Illustration of an open cavity.

Figure 3. BEM mesh for the open cavity.

Figure 4. BEM mesh for the BERIM method applied to the cavity.

Figure 5. BERIMA boundary for test horn.

Figure 6. Simulated directivity response of the test horn using BERIMA.

Figure 7. Measured directivity response of the test horn.

Figure 8. Throat resistance, comparison of BERIMA, AEBEMA and measured values.

Figure 9. Throat reactance, comparison of BERIMA, AEBEMA and measured values.

Figure 10. AEBEMA boundary for test horn.

Figure 11. Simulated directivity response of test horn using AEBEMA

Figure 12. Typical BERIM3 mesh showing surface SPL at 3kHz.

Figure 13. Comparison of computed and measured polar plots and computed SPL at the mouth.

Figure 14. BEM mesh showing sound pressure level at 3kHz.

Figure 15. Comparison of BEM results with measured data.